Accepted Manuscript

Design, synthesis and docking studies of benzimidazole derivatives as potential EGFR inhibitors

İsmail Çelik, Gülgün Ayhan-Kılcıgil, Berna Güven, Zümra Kara, A. Selen Gurkan-Alp, Arzu Karayel, Arzu Onay-Beşikci

PII: S0223-5234(19)30312-5

DOI: https://doi.org/10.1016/j.ejmech.2019.04.012

Reference: EJMECH 11247

To appear in: *European Journal of Medicinal Chemistry*

Received Date: 31 December 2018

Revised Date: 1 March 2019

Accepted Date: 4 April 2019

Please cite this article as: İ. Çelik, Güü. Ayhan-Kılcıgil, B. Güven, Zü. Kara, A.S. Gurkan-Alp, A. Karayel, A. Onay-Beşikci, Design, synthesis and docking studies of benzimidazole derivatives as potential EGFR inhibitors, *European Journal of Medicinal Chemistry* (2019), doi: https://doi.org/10.1016/j.ejmech.2019.04.012.

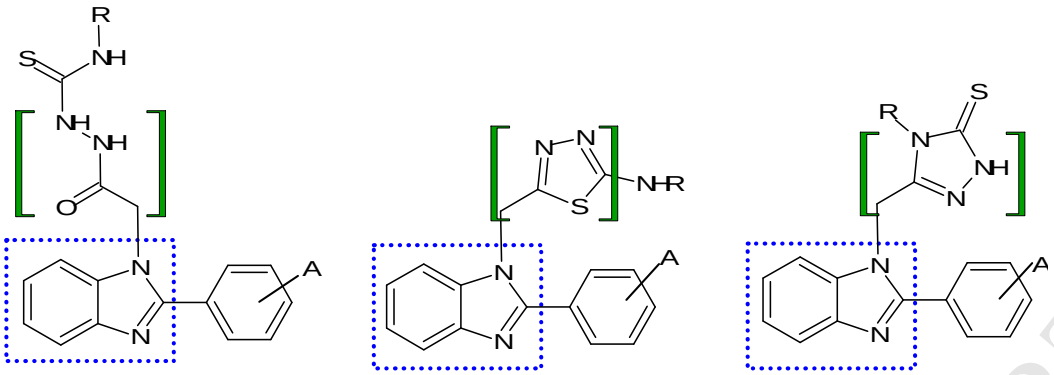

R= methyl; ethyl; 2-piperidinoethyl; 2-morpholinoethyl

A= H; 4-Cl; 4-methoxy; 3,4-dibenzyloxy

Design, Synthesis and Docking Studies of Benzimidazole Derivatives as Potential EGFR Inhibitors

İsmail Çelik[1,2], Gülgün Ayhan-Kılcıgil[1*], Berna Güven[3], Zümra Kara[3], A. Selen Gurkan-Alp[1], Arzu Karayel[4], Arzu Onay-Beşikci[3]

[1] Ankara University, Faculty of Pharmacy, Department of Pharmaceutical Chemistry, 06100 Tandoğan-Ankara/Turkey

[2] Erciyes University, Faculty of Pharmacy, Department of Pharmaceutical Chemistry, 38039 Kayseri, Turkey

[3] Ankara University, Faculty of Pharmacy, Department of Pharmacology, 06100 Tandoğan-Ankara/Turkey

[4] Hitit University, Faculty of Arts and Science Department of Physics 19030 Çorum, Turkey

Abstract

In this study, a series of benzimidazoles bearing thiosemicarbazide chain or triazole and thiadiazole rings were designed and synthesized. Crystal and molecular structure of the compound **5c** has been characterized by single crystal X-ray crystallographic analysis. EGFR kinase inhibitory potencies of synthesized compounds were compared with erlotinib *in vitro* and most of the compounds exhibited significant activities. Cell culture studies were also carried out for selected compounds and **12b** was found to be the most active compound. To understand the binding mode of synthesized benzimidazoles, three compounds (**12b, 16, 16c**) were selected and placed on the binding site of EGFR tyrosine kinase based on their kinase inhibitor potencies and cell culture studies. By docking study that compound **12b** indicated two-hydrogen bonding interactions with residues of LYS721 and THR830 at the binding pocket.

Key words: Benzimidazole, Thiosemicarbazide, Triazole, Thiadiazole, EGFR Inhibitory Activity, X-Ray, Docking

1. Introduction

Cancer is still one of the most serious diseases in the world. According to the World Health Organization (WHO), cancer is the second most important cause of deaths worldwide that had reached 8.8 million in 2015. The number of new cases per year is projected to increase from 14.1 billion in 2012 to 21.6 billion in 2030. The epidermal growth factor receptor (EGFR) belongs to ErbB family of receptor tyrosine kinases. It is upregulated in many cancers such as breast cancer and head and neck squamous cell carcinoma. Moreover, in more than half of the patients with non-small cell lung cancer (NSCLC), EGFR is overexpressed [1, 2]. Therefore, EGFR is an attractive target for anticancer therapy and a larger number of EGFR tyrosine kinase inhibitors (TKIs) have been developed [3-7]. They exert their action through competitive inhibition for adenosine triphosphate (ATP) binding in the tyrosine kinase domain. Benzimidazoles have various activities and have versatile use in medicinal chemistry. Various studies reported that a third generation EGFR inhibitor nazartinib [8], which has benzimidazole structure and the core structure of numerous biologically active compounds, always possess a wide range of bioactivities including antimicrobial [9], antiparasitic [10], antihistaminic [11], antiallergic [12], anticancer [13-16] and antioxidant [17-19] . Other third generation EGFR TKIs, avitinib [20] and osimertinib [21], that bear indolopirimidine and indol rings, respectively, are bioisosteres to benzimidazole (Figure 1) and are indicated for EGFR-mutated NSCLC.

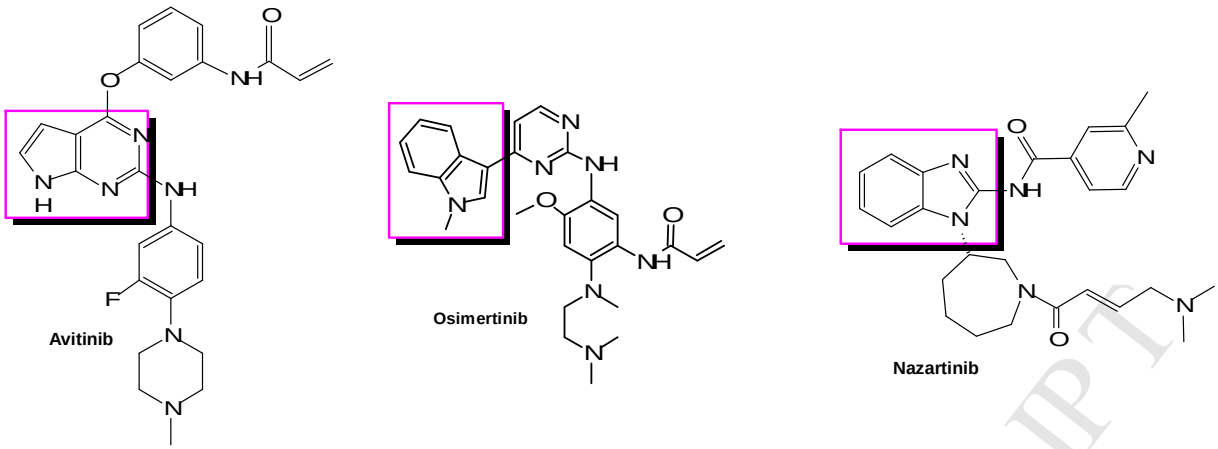

Figure 1. Third generation EGFR Inhibitors

In this study, a series of benzimidazoles with thiosemicarbazide side chain or triazole and thiadiazole rings were designed and synthesized. Next, their inhibitory potencies of EGFR kinase activity were compared to erlotinib *in vitro.*

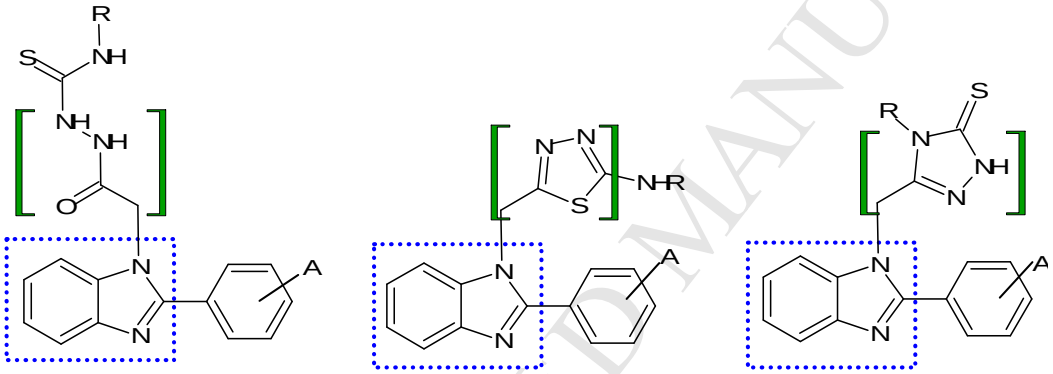

R= methyl; ethyl; 2-piperidinoethyl; 2-morpholinoethyl
A= H; 4-Cl; 4-methoxy; 3,4-dibenzyloxy

Figure 2. Designed benzimidazole derivatives

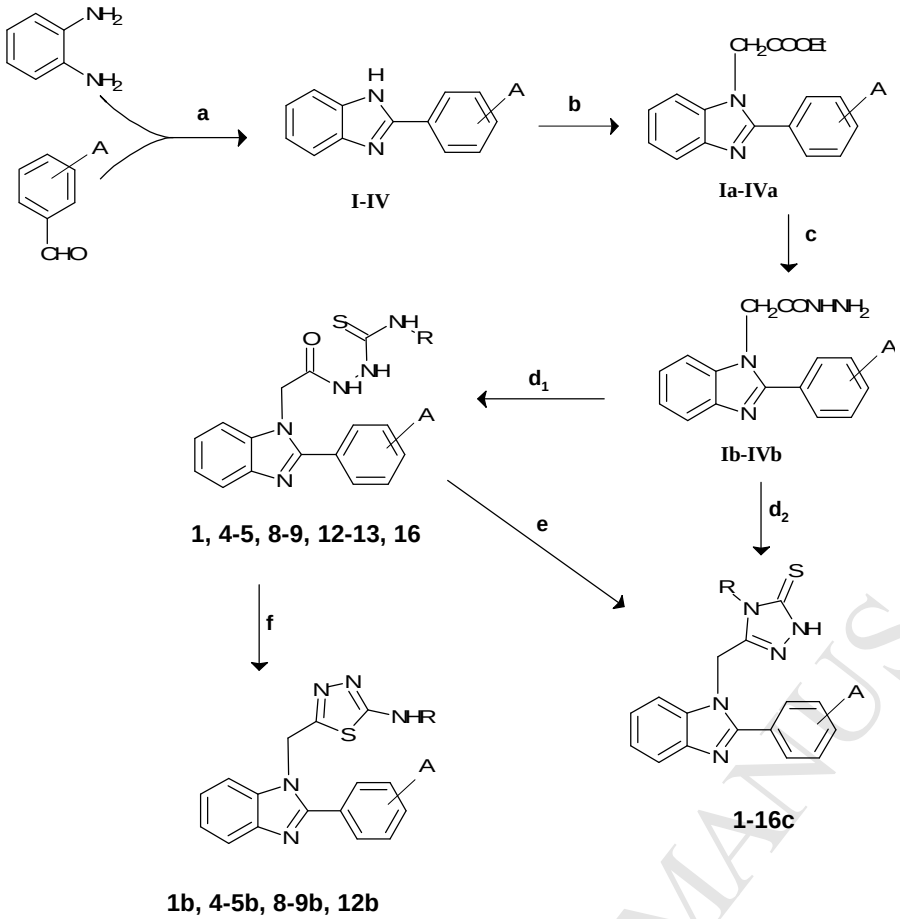

Scheme. Synthesis of benzimidazole derivatives
Reagents and conditions (a) $Na_2S_2O_5$ (b) $ClCH_2COOEt/KOH–DMSO$ (c) $NH_2NH_2.H_2O/EtOH$ (d_1) methyl/ethyl isothiocyanate-abs EtOH 3h (d_2) 2-piperidino/morpholinoethylisothiocyanate-abs EtOH 3h (e) H_2SO_4 (f) NaOH

2. Results and Discussion

2.1. Synthesis of compounds

The reaction sequences of the synthesized compounds are outlined in the **Scheme** above. Benzimidazoles (I-IV) were synthesized via oxidative condensation of *o*-phenylenediamine and benzaldehyde derivatives. 2-(2-substitutedphenyl)-*1H*-benzo[d]imidazol-l-yl) acetates (Ia-IVa) were obtained from the reaction of compounds **I-IV** with ethyl chloroacetate in KOH/DMSO. Ester compounds (**Ia-IVa**) were treated with hydrazine hydrate to give the hydrazides (**Ib-IVb**). The thiosemicarbazides were obtained from reaction of acid hydrazide with alkyl isothiocyanates in ethanol. Cyclization reaction of these compounds with sulfuric acid or sodium hydroxide resulted in the formation of thiadiazole and triazole derivatives, respectively. Surprisingly, reaction of the hydrazide derivatives with 2-piperidino and 2-morpholinoethylisothiocyanates leads directly to the triazole derivatives, in which no thiosemicarbazide derivatives can be isolated. Therefore, thiadiazole compounds containing this side chain have not been obtained. All newly synthesized compounds were characterized by ^{1}H NMR,^{13}C NMR, MS and elemental analysis data.

2.2. Biological evaluations

2.2.1. EGFR Kinase Inhibitory Activity

EGFR kinase activity was measured *in vitro* by using ADP-Glo™ assay kit. [22]. This assay determines luminescence obtained in a phosphorylation reaction where EGFR kinase, a substrate ($PolyE_4Y_1$), and ATP were present in the reaction medium. Inhibitory efficiency of each new compound was determined by comparing the enzyme activity in the presence of the inhibitors with the maximum enzyme activity. Inhibitory efficiencies of the newly synthesized compounds were then evaluated by comparing them with the known inhibitor, erlotinib (Figure 3). New compounds inhibited EGFR kinase to varying degrees (6-42%). Next, cell culture studies were carried out for selected compounds that showed an inhibitory effect of ≥30%.

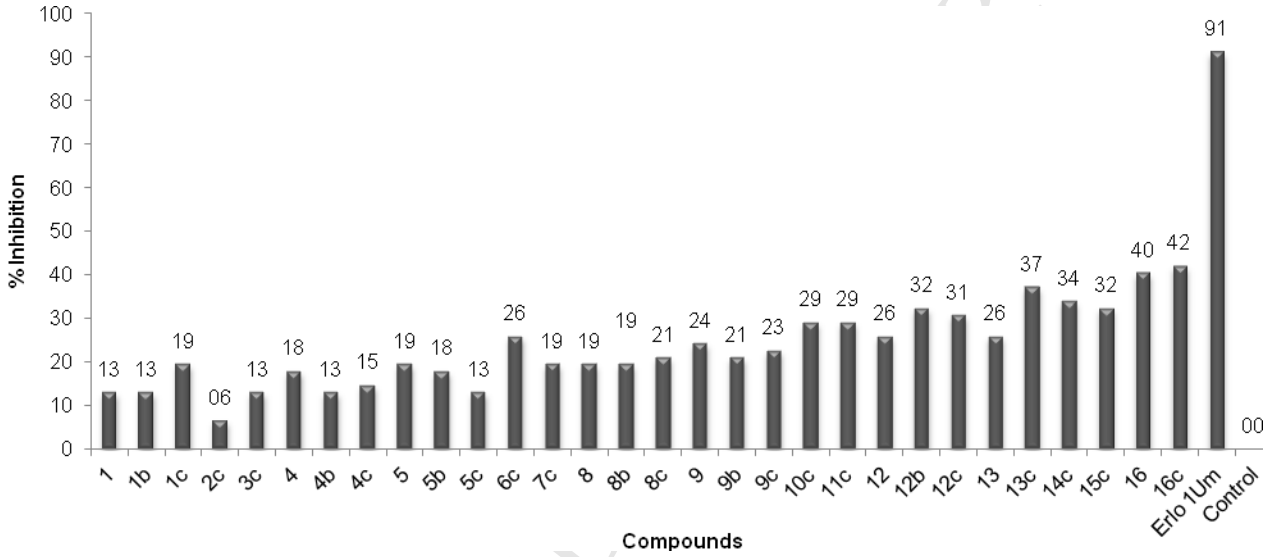

Figure 3. Percent inhibition by new compounds and erlotinib of EGFR kinase activity.

Control experiments only included DMSO and erlotinib – an inhibitor of EGFR activity- was used to validate the assay conditions.

Structure activity relationships of the synthesized compounds as EGFR kinase inhibitors have shown that the benzimidazoles having 3,4-dibenzyloxyphenyl substituents in the second position are more active than the unsubstituted/4-Cl/4-OCH3 phenyl derivatives. This can be interpreted as bulky groups increasing activity.

It has also been found that those carrying alkyl groups on the “N” such as methyl or ethyl are more active than those carrying piperidinyl or morpholinyl ethyl groups. This has shown that increasing the polarity reduces effectiveness.

When compared with the thiosemicarbazide, thiadiazole and triazole structures, it was found that most of the molecules carrying triazole structure were more active than the ones bearing the thiosemicarbazide and thiadiazole counterparts.

2.2.2. Cell Proliferation Inhibitory Activity

The MCF7 line represents differentiated mammary epithelium by its ability to process estradiol via cytoplasmic estrogen receptors in addition to expressing epidermal growth factor receptors [23, 24]. Therefore, this cell line was selected to investigate whether the new compounds affect cell proliferation and how they compare with erlotinib. In line with the superior structural relationship with EGFR receptor, only compound 12b which contains phenyl ring in the second position of benzimidazole and N-metilamino group of 1,3,4-thiadiazole ring inhibited cell proliferation by 25%.. Compound **12c** inhibited cell proliferation by about 7% however other compounds had no effect. At a concentration where EGFR kinase activity was inhibited by nearly 92%, erlotinib's inhibitory effect on cell proliferation was around **60**%. This indicates that *in vitro* inhibitory activity of EGFR kinase may not be fully translated to the inhibition of proliferation when tested on cells.

Some selected compounds were also tested against cervical cancer represented by HeLA cell line. This cell line also includes EGFR receptor and erlotinib (1 μM) inhibited kinase activity by 93% . This confirmed the sensitivity of EGFR kinase of HeLa cells to the inhibition by erlotinib. However, none of the compounds inhibited EGFR kinase activity significantly, although some inhibitory effect was observed within the range of 4-28%. (results not shown).

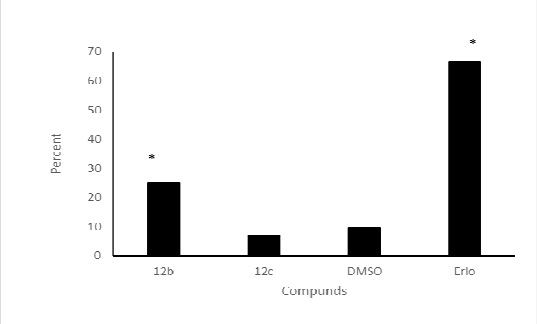

Figure 4. Percent inhibition of cell proliferation as calculated based on the amount of viable cells after inhibitor treatment.

*vs DMSO-treated cells, $p<0.05$

2.3. Molecular docking studies

In order to understand the binding mode of benzimidazole linked thiosemicarbazide, substituted triazole and thiadiazole derivatives, docking studies were carried out by using the X-ray structure of EGFR tyrosine kinase (PDB ID: 1M17), which was previously used for the development of some novel substituted benzimidazole-linked oxadiazoles [14] and some pyrazolo[3,4-*d*]pyrimidines [25] as cytotoxic agents. Three compounds were selected and docked into the binding site of EGFR tyrosine kinase (PDB ID: 1M17**)** based on their kinase inhibitor potencies (16 and 16c) and cell culture studies (12b). Amino acids in the active site of EGFR tyrosine kinase and the interaction of the best docking pose of compounds **12b, 16** and **16c** are shown in Figure 5. The docking analysis of the compounds revealed that hydrogen bonding represented by green line

with LYS721 (for all compounds studied), THR830 (only for compound **12b**) and van der Waals interactions (cyan-maroon) observed in the active site stabilize the molecules in the protein. One hydrogen bond (2.26 Å) was observed between C=O of the compound **16** and LYS721 side chain. It was observed that the compound **16** was compatible with the active binding site thanks to van der Waals interactions between the residues LEU694, LYS721, PHE699, THR766, ASP831, MET769 at the binding pocket and the molecule (Figure 5a). One hydrogen bond (2.36 Å) was also observed between NH of the triazole ring of the compound **16c** and LYS721 side chain. It was shown that compound **16c** was also settled down with the formation of van der Waals interactions between the molecule and the residues LEU694, VAL702, LYS721, PHE699, ARG817, THR766 at the active site of the enzyme (Figure 5b). Compound **12b** showed two-hydrogen bonding interactions; one hydrogen bond between S of the thiadiazole ring of the compound and LYS721, one hydrogen bond between N4 of the thiadiazole and THR830 side shain with the distances 3.74 Å and 3.15 Å, respectively. In addition, the compound **12b** was inside the protein due to van der Waals interactions between the residues LEU694, LEU768, MET769 HIS811, LEU820, GLU738, ARG817, PHE699 at the binding site and the molecule (Figure 5c).

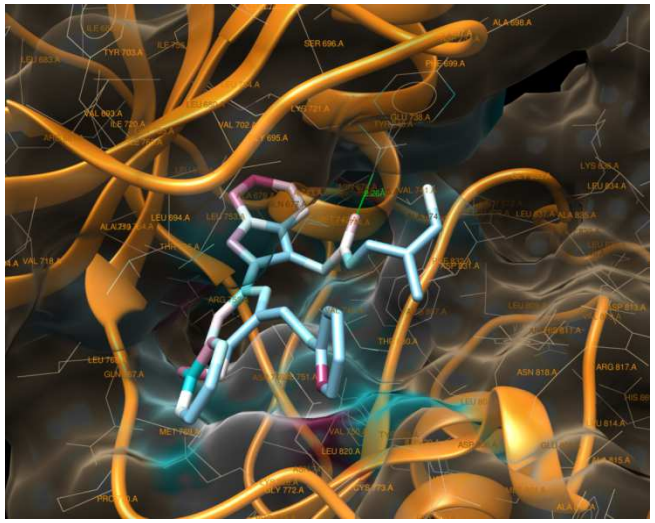

a

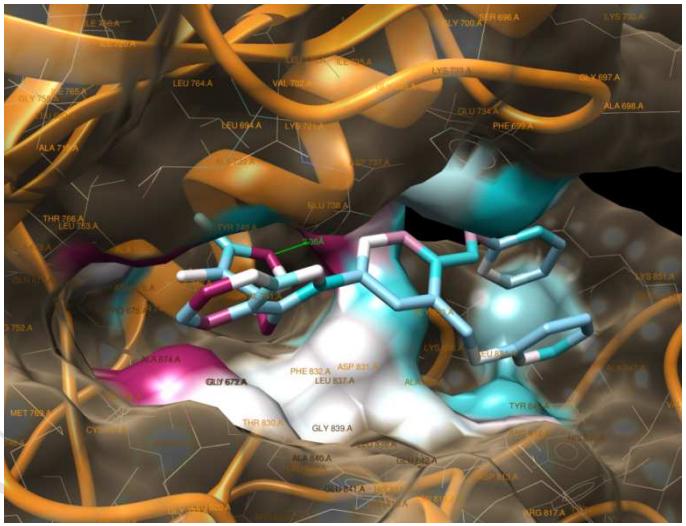

b

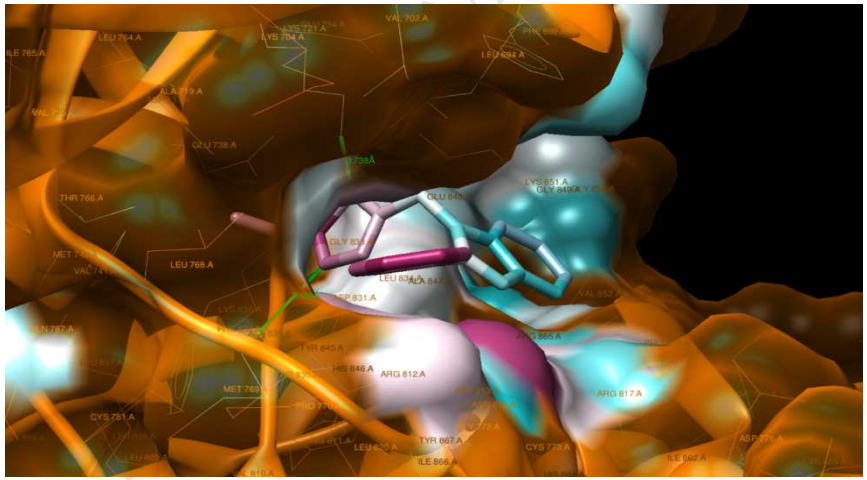

c

Figure 5. Binding mode of the most active compounds **16** (a), **16c** (b) and **12b** (c) into EGFR (PDB ID: 1M17) active site showing hydrogen bonds (green line) with LYS721 and THR830 side chain (only for compound **12b**) and van der Waals interactions (cyan-maroon). One hydrogen bond interaction between C=O (**16**) and LYS721. One hydrogen bond between triazole nitrogen (**16c**) and LYS721. Two-hydrogen bonding interactions between S of the thiadiazole (**12b**) and LYS721, and between N4 of the thiadiazole (**12b**) and THR830 side chain.

2.4. X-Ray Structure Determination

We analyzed both molecular and crystal structure of the compound **5c** (5-[(2-(4-methoxyphenyl)-1H-benzimidazole-1-yl)methyl]- 2,4-dihidro-4-ethyl-3H-1,2,4-triazole-3-thione). We determined the parameters regarding to molecular structure including the unit cell dimensions, atomic positions, bond length, angular positions of bonds and the relative displacements. In **Table 1**, we tabulated all relevant parameters as well as settings of X-ray analysis data. In **Figure 6**, we show the Ortep diagram [26] and crystal packing diagram of **5c** in unit cell.

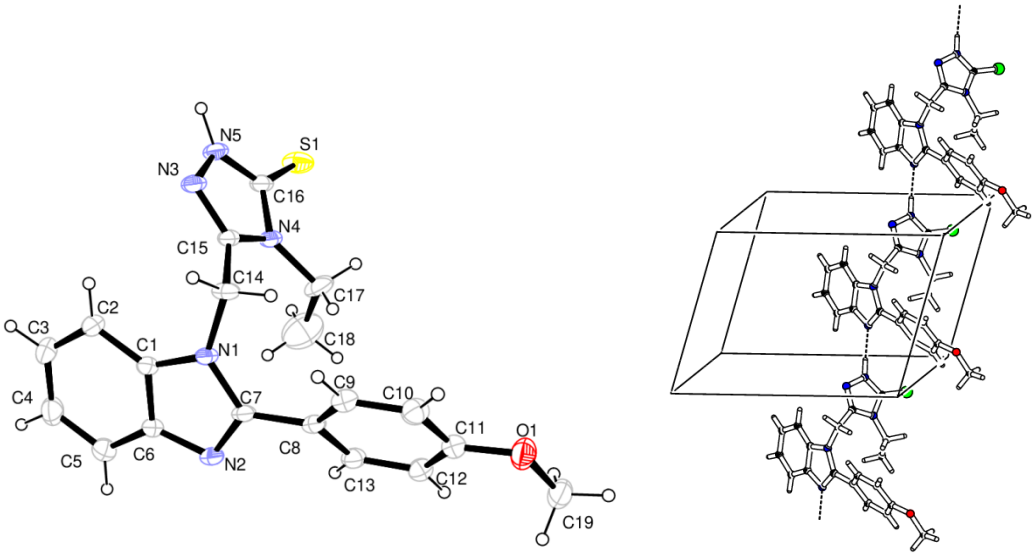

Figure 6. The ORTEP diagram of **5c** (**left**) and the crystal packing of **5c** (**right**) along [010] containing N5—H1•••N2 hydrogen bond.

The main molecule in building blocks of the compound **5c** consists of 1, 2, 4-triazole ring with ethyl and methoxyphenylbenzimidazole groups at fourth and at fifth location of this ring, respectively. Relevant molecule was crystallized in thione form. The hydrogen atoms are bound to the N5 atom instead of the S1 atom in thione tautomeric form. Moreover, the bond distances of N5–C16 (1.340(3) Å), N4–C16 (1.370(3) Å) and C16–S1(1.676(3) Å) are in value what we expected single and double bond distances for this tautomeric form.

To describe three dimensional structure of compound **5c**, we found the torsion angles of ethyl and methoxyphenylbenzimidazole groups by the triazole ring. We determined the rotation of the ethyl with respect to triazole ring with the torsion angle of C16–N4–C17–C18 which is found to be [-87.7(5)º]. The rotation of benzimidazolemethyl group with respect to triazole ring can be described by two torsion angles; N1–C14–C15–N4 (-63.8(4)º) and C1–N1–C14–C15 (-59.0(3)º). Additionally, the angular positioning of the methoxyphenyl ring with respect to benzimidazole ring is given by the

torsion angles of N2–C7–C8–C9 (-148.2(3)º). We listed some of the specific geometric parameters in **Table 2**.

We can say that the benzimidazole counterpart of the structure is almost planar as the dihedral angle connecting the imidazole and the adjacent phenyl rings is 0.90(9)°. While the dihedral angle joining benzimidazole ring and the methoxyphenyl ring is 34.94(8)º, the dihedral angle between triazole ring plane and benzimidazole group is 87.59(8)º. This result clearly demonstrates that the triazole part of the molecule is almost perpendicular to the benzimidazole moieties.

In addition, triazole ring is also planar. The deviation of C16 atom from this plane is 0.0034 Å, while the deviation of the thione group bonded to C16 from the triazole plane is 0.0223 Å. The deviation of C17 bonded to triazole ring is 0.1020 Å. The maximum deviation from the mean plane of the benzimidazole ring for C2 is -0.0106 Å (for C4 0.0158 Å). The deviation of C9 from the mean plane of phenyl ring connected to benzimidazole ring is -0.0098 Å, while the deviation of O1 bonded to phenyl ring is 0.0415 Å.

Table 1. The list of parameters of compound **5c** related to crystal data and structure refinement.

Crystal data	**5c**
Chemical Formula	$C_{19}H_{19}N_5O_1S_1$
System, sp. gr., *Z*	Triclinic, P -1, 2
a, *b*, *c*, Å	8.5407(6),9.0142(6),13.2882(11)
α, β, γ, deg	102.055(4),95.180(5),112.763(4)
V, Å^3	905.8
D_x, g cm^{-3}	1.34
Radiation, λ, Å	MoK_α, 0.71073
μ, mm^{-1}	0.197
T, K	296(2)
Sample size, mm	0.69 x 0.52 x 0.32
Diffractometer	Bruker APEX2
Scan mode	ω - 2θ
Absorption correction,T_{min}, T_{max}	Psi-scan, 0.876, 0.9396
θ_{max}, deg	28.57
h, *k*, *l* ranges	-11≤ h ≤11,-12 ≤ k ≤12, -16≤ l ≤17
Number of reflections:measured/unique(*N*1)	20512/4551
R_{int}/with $I > 2\sigma(I)$ (*N*2)	0.0455/3280
Refinement method	full-matrix least square in F^2
Number of refined parameters	257
*wR*2 relative to *N*1	0.218
*R*1 relative to *N*2	0.069
Goodness-of-fit on F^2	1.058
Δρmax/Δρmin, e/Å^3	0.531/-0.581

Table 2. Bond lengths (Å) , bond angles and torsion angles (°) of current molecule.

Bond distances			
C19 – O1	1.424(4)	N5 – C16	1.340(3)
S1 – C16	1.676(3)	N5 – N3	1.370(3)
N1– C7	1.381(3)	N3 – C15	1.298(3)
N1 – C1	1.392(4)	N4 – C15	1.367(3)
N1 – C14	1.457(3)	N4 – C16	1.370(3)
N2 – C7	1.324(3)	O1 – C11	1.364(4)
N2 – C6	1.388(3)		
Bond angles			
C7 – N1 – C1	106.6(2)	N2 – C6 – C5	130.5(2)
C1 – N1 – C14	123.5(2)	N2 – C7 – N1	111.6(2)
C7 – N2 – C6	106.4(2)	N2 – C7 – C8	122.4(2)
C16 – N5 – N3	113.1(2)	N5 – C16 – N4	103.7(2)
C15 – N4 – C16	107.7(2)	N5 – C16 – S1	128.9(2)
N1– C1 – C6	106.0(2)	N3 – C15 – N4	111.4(2)
C11 – O1 – C19	117.5(2)	O1 – C11 – C10	116.5(3)
N1 – C1 – C2	131.4(2)		
Torsion angles			
C16 – N5 – N3 – C15	-0.5(3)	C19 – O1 – C11 – C10	173.8(3)
N3 – N5 – C16 – N4	0.6(3)	N1 – C14 – C15 – N3	121.2(3)
N3 – N5 – C16 – S1	-179.0(2)	O1 – C11 – C10 – C9	179.0(3)
C9 – C8 – C7 – N2	-148.2(3)	C7 – N1 – C1 – C6	-0.2(3)
C13 – C8 – C7 – N1	-141.8(3)		

Hydrogen-bonding analysis revealed that current molecule has an intermolecular N–H···N hydrogen bond between N2 atom of imidazole ring and N5 atom of triazole ring of neighbor molecule shown in **Table 3**. We conclude N–H···N type hydrogen bond is the most effective onefor crystal stabilization (**Figure 6**).

Table 3. Hydrogen-bonding analysis of the relevant molecule (Å, °).

D – H ···A	**D– H**	**H ···A**	**D ···A**	**D – H ···A**
N(5) – H(1)….N(2)(i)	0.95(4)	1.87(4)	2.808(4)	172(4)

Symmetry code: (i) x, 1+y, z

Conclusion

A series of benzimidazole derivatives bearing thiosemicarbazide side chain or triazole and thiadiazole rings were synthesized. Their EGFR kinase inhibitory efficiency was determined by comparing them with a known kinase inhibitor erlotinib *in vitro* and most of the compounds exhibited significant activities. Cell culture studies were also carried out for selected compounds (12b, 12c, 13c, 14c, 15c, 16 and 16c) which exhibited EGFR kinase inhibitory activities over ≥30%) against MCF7 cell and 12b was found to be the most active compound. This situation also supported by docking study that compound 12b indicated two-hydrogen bonding interactions with residues of LYS721 and THR830 at the binding pocket while other compounds show only one interaction with LYS721 side chain.

3. Experimental

3.1. Chemistry

Uncorrected melting points were measured on a Büchi B-540 and an Electrothermal capillary melting point apparatus. All chemical reagents were purchased from E. Merck and Aldrich. ^{1}H and ^{13}C NMR spectra were recorded on Varian Varian Mercury 400 MHz instrument (Varian Inc., Palo Alto, CA, USA) at a proton resonance frequency of 400.1779 and 100.6243 MHz for carbon . Chemical shifts are given in parts per million (ppm) relative to tetramethylsilane as an internal standard. The following abbreviations are used to identify peak splitting patterns; br = broad, s = singlet, d = doublet, t = triplet, q = quartet, dd =doublet of doublet, m =multiplet. Coupling constant (J) are reported in Hz. ES-MS were taken with a Waters ZQ Micromass LC–MS spectrometer with positive electrospray ionization method. Elemental analyses (C, H, N,and S) were performed by Leco CHNS 932 instrument. All instrumental analyses were carried out at The Central Instrumentation Laboratory of the Pharmacy Faculty of Ankara University, Ankara, Turkey.

Compounds I-IV, Ia-IVa, Ib-IIIb have been synthesized [27] and compound IVb in our laboratory previously.

3.1.1. Preparation of thiosemicarbazides N-methyl/ethyl-2-(2-(2-(phenyl/substitutedphenyl-1*H*-benzo[d]imidazol-1-yl)acetyl)hydrazine-1-carbothioamides (1, 4-5, 8-9, 12-13, 16).

The mixture of acid hydrazide (2.03 mmol) and alkyl isothiocyanate (3.05 mmol) in absolute ethanol (20mL) were refluxed for 3 h. The precipitate formed by cooling was filtered and crystallized from ethanol or isopropanol.

3.1.1.1. 2-{[2-(4-Chlorophenyl)-1*H*-benzimidazol-1-yl]acetyl}-*N*-ethylhydrazinecarbothioamide (1)

Yield 88%, Mp: 234°C. ^{1}H NMR (400 MHz, DMSO-d_6, ppm) δ: 1.09(t, 3H, $CH_2\underline{CH_3}$), 3.47-3.51 (m, 2H, $\underline{CH_2}CH_3$), 4.97 (s, 2H, CH_2), 7.26-7.32 (m, 2H, Ar-H), 7.53-7.79 (m, 6H, Ar-H), 8.08, 8.71, 9.32, 9.54, 9.73, 10.30 (brs, NH). MS (ESI+) *m/z*: 388.01 (M+H), 390.15 (M+2+H). Anal. for $C_{18}H_{18}ClN_5OS$ (%) Calcd/Found: C 55.74/55.40; H 4.68/4.84; N 18.06/17.76; S 8.27/8.104

3.1.1.2. 2-{[2-(4-Chlorophenyl)-1*H*-benzimidazol-1-yl]acetyl}-*N*-methylhydrazinecarbothioamide (4)

Yield 83%, Mp: 244°C. ^{1}H NMR (400 MHz, DMSO-d_6, ppm) δ: 2.91(d, 3H, CH_3), 4.96 (s, 2H, CH_2), 7.26-7.33 (m, 2H, Ar-H), 7.52-7.79 (m, 6H, Ar-H), 8.10, 8.65, 9.40, 9.61, 9.77, 10.32 (brs, NH). MS (ESI+) *m/z*: 373.94 (M+H), 375.95 (M+2+H). Anal. for $C_{17}H_{16}ClN_5OS$ (%) Calcd/Found: C 54.61/54.38; H 4.31/4.46; N 18.73/18.42; S 8.58/8.481

3.1.1.3. *N*-Ethyl-2-{[2-(4-methoxyphenyl)-1*H*-benzimidazol-1-yl]acetyl}- hydrazinecarbothioamide (5)

Yield 78%, Mp: 215°C. ^{1}H NMR (400 MHz, DMSO-d_6, ppm) δ: 1.09 (t, 3H, $CH_2\underline{CH_3}$), 3.47-3.52 (m, 2H, $\underline{CH_2}CH_3$), 3.85 (s, 3H, OCH_3), 4.94 (s, 2H, CH_2), 7.10 (d, 2H, Jo= 8.8 Hz, Ar-H), 7.21-7.27 (m, 2H, Ar-H), 7.42-7.52 (m, 1H, Ar-H), 7.62-7.73 (m, 3H, Ar-H), 7.97, 8.60, 9.26, 9.63, 10.22 (brs, NH). MS (ESI+) *m/z*: 384.01(M+H). Anal. for $C_{19}H_{21}N_5O_2S$ (%) Calcd/Found: C 59.51/59.13; H 5.52/5.81; N 18.26/18.02; S 8.36/8.21

3.1.1.4. 2-{[2-(4-Methoxyphenyl)-1*H*-benzimidazol-1-yl]acetyl}-*N*-methylhydrazinecarbothioamide (8)

Yield 87%, Mp: 221°C. ^{1}H NMR (400 MHz, DMSO-d_6, ppm) δ: 2.92 (d, 3H, CH_3), 3.85 (s, 3H, OCH_3), 4.94 (s, 2H, CH_2), 7.11 (dd, 2H, Jo=8.8Hz, Jm=2.4 Hz, Ar-H), 7.22-7.28 (m, 2H, Ar-H), 7.49-7.51 (m, 1H, Ar-H), 7.61-7.71 (m, 3H, Ar-H), 8.08, 8.63, 9.40, 9.61, 9.74, 10.29 (brs, NH). MS (ESI+) *m/z*: 370.03 (M+H). Anal. for $C_{18}H_{19}N_5O_2S.0.9\ H_2O$ (%) Calcd/Found: C 56.07/55.88; H 5.39/5.70; N 18.17/17.97; S 8.31/8.339.

3.1.1.5. *N*-Ethyl-2-[(2-phenyl-1*H*-benzimidazol-1-yl)acetyl]hydrazinecarbothioamide (9)

Yield 81%, Mp: 220°C. ^{1}H NMR (400 MHz, DMSO-d_6, ppm) δ: 1.09 (t, 3H, $CH_2\underline{CH_3}$), 3.47-3.51 (m, 2H, $\underline{CH_2}CH_3$), 4.97 (s, 2H, CH_2), 7.26-7.29 (m, 2H, Ar-H), 7.52-7.58 (m, 4H, Ar-H), 7.69-7.77 (m, 3H, Ar-H), 8.08, 8.69, 9.33, 9.55, 9.71, 10.22 (brs, NH). MS (ESI+) *m/z*: 354.02 (M+H). Anal. for $C_{18}H_{19}N_5OS$ (%) Calcd/Found: C 61.17/61.06; H 5.38/5.55; N 19.83/19.42; S 9.07/8.92.

3.1.1.6. *N*-Methyl-2-[(2-phenyl-1*H*-benzimidazol-1-yl)acetyl]hydrazinecarbothioamide (12)

Yield 80%, Mp: 210°C. ^{1}H NMR (400 MHz, DMSO-d_6, ppm) δ: 2.91(d, 3H, CH_3), 4.96 (s, 2H, CH_2), 7.24-7.32 (m, 2H, Ar-H), 7.52-7.59 (m, 4H, Ar-H),7.67-7.76 (m, 3H, Ar-H), 8.08, 8.64, 9.41, 9.61, 9.74, 10.29 (brs, NH). MS (ESI+) *m/z*: 340.05 (M+H). Anal. for $C_{17}H_{17}N_5OS$ (%) Calcd/Found: C 60.16/59.76; H 5.05/5.28; N 20.63/20.23; S 9.45/9.39.

3.1.1.7. 2-{[2-(3,4-Dibenzyloxyphenyl)-1*H*-benzimidazol-1-yl]acetyl}-*N*-ethylhydrazinecarbothioamide (13)

Yield 69%, Mp: 170°C. ^{1}H NMR (400 MHz, DMSO-d_6, ppm) δ: 1.05 (t, 3H, $CH_2\underline{CH_3}$), 3.41-3.48 (m, 2H, $\underline{CH_2}CH_3$), 4.70 (s, 2H, CH_2), 5.18 (s, 2H, OCH_2Ph), 5.22 (s, 2H, OCH_2Ph), 7.19-7.23 (m, 4H, Ar-H), 7.28-7.84

(m, 16H, Ar-H, NH), MS (ESI+) *m/z*: 565.98 (M+H). Anal. for $C_{32}H_{31}N_5O_3S$-0.5H_2O (%) Calcd/Found: C 66.87/66.78; H 5.61/5.72; N 12.19/12.32; S 5.58/5.41.

3.1.1.8. 2-{[2-(3,4-Dibenzyloxyphenyl)-1*H*-benzimidazol-1-yl]acetyl}-*N*-methylhydrazinecarbothioamide (16)

Yield 72%, Mp: 160°C. ^{1}H NMR (400 MHz, DMSO-d_6, ppm) δ: 3.89 (d, 3H, CH_3), 4.98 (s, 2H, CH_2), 5.18 (s, 2H, O*CH*$_2$Ph), 5.24 (s, 2H, O*CH*$_2$Ph), 7.20-7.49 (m, 15H, Ar-H), 7.54 (d, Jm=2 Hz, Ar-H),7.67 (dd, Jo=6.8 Hz, Jm=2.0 Hz, Ar-H), 8.03, 9.38, 9.59, 9.69, 10.29 (brs, NH). MS (ESI+) *m/z*: 551.97 (M+H). Anal. for $C_{31}H_{29}N_5O_3S$. H_2O (%) Calcd/Found: C 65.37/65.29; H 5.44/5.02; N 12.30/12.18; S 5.69/5.93

3.1.2. Preparation of the N-alkyl-5-((2-phenyl/substitutedphenyl-1*H*-benzo[d]imidazol-1-yl)methyl)-1,3,4-thiadiazol-2-amines (1b, 4b-5b, 8b-9b, 12b).

Thiosemicarbazides (3.4 mmol) were stirred in concentrated sulfuric acid (10 mL) for 10 min in ice bath and then continued stirring at room temperature for another 10 min. At the end of this period the solution was poured slowly into ice water and pH was made alkaline (pH=8) with the aqueous ammonia. The precipitate was separated by filtration and washed with water. The crude product was purified through crystallization with ethanol or ethanol / isopropanol (10:1)

3.1.2.1. 5-{[2-(4-Chlorophenyl)-1*H*-benzimidazol-1-yl]methyl}-*N*-ethyl-1,3,4-thiadiazol-2-amine (1b)

Yield 42%, Mp: 176-177°C. ^{1}H NMR (400 MHz, DMSO-d_6, ppm) δ: 1.10 (t, 3H, $CH_2\underline{CH_3}$), 3.16-3.23 (m, 2H, $\underline{CH_2}CH_3$), 5.75 (s, 2H, CH_2), 7.27-7.34 (m, 2H, Ar-H), 7.64-7.73 (m, 5H, Ar-H, N-H), 7.88 (d, 2H, Jo=8.8 Hz, Ar-H). MS (ESI+) *m/z*: 370.03 (M+H), 372.4 (M+2+H). Anal. for $C_{18}H_{16}ClN_5S$ (%) Calcd/Found: C 58.45/58.17; H 4.36/4.05; N 18.93/18.82; S 8.67/8.48

3.1.2.2. 5-{[2-(4-Chlorophenyl)-1*H*-benzimidazol-1-yl]methyl}-*N*-methyl-1,3,4-thiadiazol-2-amine (4b)

Yield 51%, Mp: 234-237°C. ^{1}H NMR (400 MHz, DMSO-d_6, ppm) δ: 2.79 (d, 3H, CH_3), 5.75 (s, 2H, CH_2), 7.14-7.34 (m, 2H, Ar-H), 7.65-7.73 (m, 5H, Ar-H, N-H), 7.87 (d, 2H, Jo=8.8 Hz, Ar-H). MS (ESI+) *m/z*: 356.2 (M+H), 358.3 (M+2+H). Anal. for $C_{17}H_{14}ClN_5S$-1.6H_2O (%) Calcd/Found: C 53.07/52.78; H 4.50/4.68; N 18.20/18.70; S 8.33/7.93.

3.1.2.3. *N*-Ethyl-5-{[2-(4-methoxyphenyl)-1*H*-benzimidazol-1-yl]methyl}-1,3,4-thiadiazol-2-amine (5b)

Yield 38%, Mp: 189-191°C. ^{1}H NMR (400 MHz, DMSO-d_6, ppm) δ: 1.09 (t, 3H, $CH_2\underline{CH_3}$), 3.19-3.23 (m, 2H, $\underline{CH_2}CH_3$), 3.84 (s, 3H, OCH_3), 5.71 (s, 2H, CH_2), 7.13 (d, 2H, Jo=8.8 Hz, Ar-H), 7.23-7.30 (m, 2H, Ar-H), 7.60-7.71 (m, 3H, Ar-H, N-H), 7.80 (d, 2H, Jo=8.4 Hz, Ar-H). ^{13}C NMR (100 MHz, DMSO-d_6, ppm) δ: 14.06, 39.41, 43.15, 55.27, 110.76, 114.24, 118.96, 121.84, 122.27, 122.45, 130.65, 135.42, 142.53, 152.59, 152.80,

160.47, 168.97. MS (ESI+) *m/z*: 352.0 (M+H). Anal. for $C_{19}H_{19}N_5OS$ (%) Calcd/Found: C 62.44/62.10; H 5.24/5.51; N 19.16/18.81; S 8.77/8.74.

3.1.2.4. 5-{[2-(4-Methoxyphenyl)-1*H*-benzimidazol-1-yl]methyl}-*N*-methyl-1,3,4-thiadiazol-2-amine (8b)

Yield 35%, Mp: 194°C. ^{1}H NMR (400 MHz, DMSO-d_6, ppm) δ: 2.78 (d, 3H, CH_3), 3.84 (s, 3H, OCH_3), 5.71 (s, 2H, CH_2), 7.13 (d, 2H, Jo=8.4 Hz, Ar-H), 7.23-7.30 (m, 2H, Ar-H), 7.60-7.69 (m, 3H, Ar-H, N-H), 7.79 (d, 2H, Jo=8.8, Ar-H). MS (ESI+) *m/z*: 352.00 (M+H). Anal. for $C_{18}H_{17}N_5OS$-1.0 H_2O (%) Calcd/Found: C 58.51/58.42; H 5.18/5.11; N 18.95/19.35; S 8.68/9.43.

3.1.2.5. *N*-Ethyl-5-[(2-phenyl-1*H*-benzimidazol-1-yl)methyl]-1,3,4-thiadiazol-2-amine (9b)

Yield 44%, Mp: 105-107.5°C. ^{1}H NMR (400 MHz, DMSO-d6, ppm) δ: 1.09 (t, 3H, $CH_2\underline{CH_3}$), 3.18-3.21 (m, 2H, $\underline{CH_2}CH_3$), 5.73 (s, 2H, CH_2), 7.30-7.31 (m, 2H, Ar-H), 7.58-7.71 (m, 6H, Ar-H, N-H), 8.84 (s, 2H, Ar-H). MS (ESI+) *m/z*: 336.5 (M+H). Anal. for $C_{18}H_{17}N_5S$ (%) Calcd/Found: C 64.45/64.47; H 5.10/5.32; N 20.87/20.48; S 9.55/9.22.

3.1.2.6. *N*-Methyl-5-[(2-phenyl-1*H*-benzimidazol-1-yl)methyl]-1,3,4-thiadiazol-2-amine (12b)

Yield 53%, Mp: 109-112.5°C. ^{1}H NMR (400 MHz, DMSO-d_6, ppm) δ: 2.79 (d, 3H, CH_3), 5.73 (s, 2H, CH_2), 7.26-7.33 (m, 2H, Ar-H), 7.57-7.59 (m, 3H, Ar-H, N-H), 7.62 (d, 2H, Jo=7.2 Hz, Ar-H), 7.72 (d, 1H, Jo=7.2 Hz, Ar-H), 7.82-7.85 (m, 2H, Ar-H). MS (ESI+) *m/z*: 322.4 (M+H). Anal. for $C_{17}H_{15}N_5S$-0,7H_2O (%) Calcd/Found: C 61.13/60.97; H 4.94/4.82; N 20.96/21.36; S 9.60/9.98.

3.1.3. Preparation of 4-alkyl-5-((2-phenyl/substitutedphenyl -1*H*-benzo[d]imidazol-1-yl)methyl)-2,4-dihydro-3H-1,2,4-triazole-3-thione (1c-16c).

3.1.3.a. Compounds 1c, 4c-5c, 8c-9c, 12c-13c, 16c

Thiosemicarbazides (3.4 mmol) (1,4-5,8-9,12-13,16) in 1 N sodium hydroxide (10 mL) were refluxed for 1 h, then the mixture was cooled and acidified to pH 6 with 1 N hydrochloric acid. Precipitate formed was filtered, washed with water. The solid was crystallized from ethanol.

3.1.3.a.1. 5-{[2-(4-Chlorophenyl)-1*H*-benzimidazol-1-yl]methyl}-4-ethyl-2,4-dihydro-3*H*-1,2,4-triazole-3-thione (1c)

Yield 48%, Mp: 279-280°C. ^{1}H NMR (400 MHz, DMSO-d_6, ppm) δ: 1.00 (t, 3H, $CH_2\underline{CH_3}$), 3.85-3.90 (m, 2H, $\underline{CH_2}CH_3$), 5.75 (s, 2H, CH_2), 7.26-7.32 (m, 2H, Ar-H), 7.54-7.64 (m, 6H, Ar-H), 13.64 (s, 1H, N-H). MS (ESI+) *m/z*: 369.95 (M+H), 371.95 (M+2+H). Anal. for $C_{18}H_{16}ClN_5S$-1.25 H_2O (%) Calcd/Found: C 55.22/54.89; H 4.73/4.13; N 17.88/17.79; S 8.19/7.95.

3.1.3.a.2. 4-Methyl-5-{[2-(4-chlorophenyl)-1*H*-benzimidazol-1-yl]methyl}-2,4-dihydro-3*H*-1,2,4-triazole-3-thione (4c)

Yield 61%, Mp: 270°C. ^{1}H NMR (400 MHz, DMSO-d_6, ppm) δ: 3.42 (s, 3H, CH_3), 5.75 (s, 2H, CH_2), 7.32-7.34 (m, 2H, Ar-H), 7.64-7.68 (m, 3H, Ar-H), 7.74-7.79 (m, 3H, Ar-H), 13.67 (s, 1H, N-H). MS (ESI+) *m/z*: 356.2 (M+H), 358.3 (M+2+H). Anal. for $C_{17}H_{14}ClN_5S$ (%) Calcd/Found: C 57.38/57.19; H 3.97/4.14; N 19.68/19.26; S 9.01/8.76.

3.1.3.a.3. 4-Ethyl-5-{[2-(4-methoxyphenyl)-1*H*-benzimidazol-1-yl]methyl}-2,4-dihydro-3*H*-1,2,4-triazole-3-thione (5c)

Yield 53%, Mp: 275-276°C. ^{1}H NMR (400 MHz, DMSO-d_6, ppm) δ: 0.93 (t, 3H, $CH_2\underline{CH_3}$), 3.79-3.85 (m, 2H, $\underline{CH_2}CH_3$), 3.87 (s, 3H, OCH_3), 5.65 (s, 2H, CH_2), 7.09-7.14 (m, 2H, Ar-H), 7.28-7.46 (m, 2H, Ar-H), 7.47-7.51 (m, 1H, Ar-H), 7.63-7.69 (m, 3H, Ar-H). ^{13}C NMR (100 MHz, DMSO-d_6, ppm) δ: 11.95, 29.26, 39.93, 54.56, 110.38, 114.18, 118.38, 120.97, 122.86, 123.15, 130.55, 135.31, 141.85, 148.17, 154.06, 161.67, 168.26. MS (ESI+) *m/z*: 366.03 (M+H). Anal. for $C_{19}H_{19}N_5OS$-0,15H_2O (%) Calcd/Found: C 61.98/61.70; H 5.28/5.29; N 19.02/19.49; S 8.70/8.85.

3.1.3.a.4. 5-{[2-(4-Methoxyphenyl)-1*H*-benzimidazol-1-yl]methyl}-4-methyl-2,4-dihydro-3*H*-1,2,4-triazole-3-thione (8c)

Yield 56%, Mp: 284°C. ^{1}H NMR (400 MHz, DMSO-d_6, ppm) δ: 3.42 (s, 3H, CH_3), 3.84 (s, 3H, OCH_3), 5.74 (s, 2H, CH_2), 7.14-7.16 (m, 2H, Ar-H), 7.33-7.35 (m, 2H, Ar-H), 7.65-7.75 (m, 4H, Ar-H), 13.67 (s, 1H, N-H). ^{13}C NMR (100 MHz, DMSO-d_6, ppm) δ: 29.86, 55.30, 110.84, 114.31, 118.96, 121.82, 122.32, 122.43, 130.44, 135.87, 142.49, 148.50, 153.19, 160.49, 167.53. MS (ESI+) *m/z*: 352.5 (M+H). Anal. for $C_{18}H_{17}N_5OS$-0.2H_2O (%) Calcd/Found: C 60.89/60.88; H 4.93/5.11; N 19.72/19.77; S 9.03/9.01.

3.1.3.a.5. 4-Ethyl-5-[(2-phenyl-1*H*-benzimidazol-1-yl)methyl]-2,4-dihydro-3*H*-1,2,4-triazole-3-thione (9c)

Yield 88%, Mp: 290°C. ^{1}H NMR (400 MHz, DMSO-d_6, ppm) δ: 0,98 (t, 3H, $CH_2\underline{CH_3}$), 3.83-3.88 (m, 2H, $CH_2\underline{CH_3}$), 5.74 (s, 2H, CH_2), 7.27-7.31 (m, 2H, Ar-H), 7.54-7.58 (m, 4H, Ar-H), 7.71-7.73 (m, 3H, Ar-H). ^{13}C NMR (100 MHz, DMSO-d_6, ppm) δ: 12.86, 38.29, 39.90, 110.81, 119.21, 122.32, 122.80 128.76, 128.86, 129.50, 129.95, 135.77, 142.35, 147.67, 153.00, 168.85. MS (ESI+) *m/z*: 336.3 (M+H). Anal. for $C_{18}H_{17}N_5S$-0,2H_2O (%) Calcd/Found: C 63.76/63.98; H 5.17/5.64; N 20.66/20.58; S 9.45/9.55.

3.1.3.a.6. 4-Methyl-5-[(2-phenyl-1*H*-benzimidazol-1-yl)methyl]-2,4-dihydro-3*H*-1,2,4-triazole-3-thione (12c)

Yield 38%, Mp: 262-263°C. ^{1}H NMR (400 MHz, DMSO-d_6, ppm) δ: 2.49 (s, 3H, CH_3), 5.70 (s, 2H, CH_2), 7.26-7.28 (m, 2H, Ar-H), 7.55-7.58 (m, 4H, Ar-H), 7.71-7.75 (m, 3H, Ar-H), 13.62 (s, 1H, N-H). ^{13}C NMR

(100 MHz, DMSO-d_6, ppm) δ: 29.78, 39.99, 110.93, 119.13, 122.30, 122.66, 128.75, 129.55, 129.86, 135.78, 142.38, 148.35, 153.10, 167.44. MS (ESI+) *m/z*: 322.3 (M+H). Anal. for $C_{17}H_{15}N_5S$ (%) Calcd/Found: C 63.52/63.48; H 4.70/4.63; N 21.79/21.61; S 9.97/9.75.

3.1.3.a.7. 5-{[2-(3,4-Dibenzyloxyphenyl)-1*H*-benzimidazol-1-yl]methyl}-4-ethyl-2,4-dihydro-3*H*-1,2,4-triazole-3-thione (13c)

Yield 36%, Mp: 268-270°C. ^{1}H NMR (400 MHz, DMSO-d_6, ppm) δ: 0,93 (t, 3H, $CH_2\underline{CH_3}$), 3.79-3.84 (m, 2H, $\underline{CH_2}CH_3$), 5.15 (s, 2H, $O\underline{CH_2}Ph$), 5.22 (s, 2H, $O\underline{CH_2}Ph$), 5.71 (s, 2H, CH_2), 7.24-7.50 (m, 14H, Ar-H), 7.55-7.57 (m, 2H, Ar-H), 7.70-7.73 (m, 1H, Ar-H), 13.72 (s, 1H, N-H). MS (ESI+) *m/z*: 548.7 (M+H). Anal. for $C_{32}H_{29}N_5O_2S$-1.5H_2O (%) Calcd/Found: C 66.87/66.84; H 5.61/5.236; N 12.18/12.18; S 5.57/5.33.

3.1.3.a.8. 5-{[2-(3,4-Dibenzyloxyphenyl)-1*H*-benzimidazol-1-yl]methyl}-4-methyl-2,4-dihydro-3*H*-1,2,4-triazole-3-thione (16c)

Yield 34%, Mp: 238°C. ^{1}H NMR (400 MHz, DMSO-d_6, ppm) δ: 3.43 (s, 3H, CH_3), 5.15 (s, 2H, $O\underline{CH_2}Ph$), 5.26 (s, 2H, $O\underline{CH_2}Ph$), 5.86 (s, 2H, CH_2), 7.30-7.58 (m, 15H, Ar-H), 7.83-7.91 (m, 2H, Ar-H), 13.77 (s, 1H, N-H). MS (ESI+) *m/z*: 534.4 (M+H). Anal. for $C_{31}H_{27}N_5O_2S$-2,55H_2O (%) Calcd/Found: C 64.24/64.30; H 5.58/5.37; N 12.08/11.85; S 5.53/5.43.

3.1.3.b. Compounds 2c-3c, 6c-7c, 10c-11c, 14c-15c

Acid hydrazide (2.03 mmol) in absolute ethanol:N,N-dimethylformamide (1:1) (20 mL) and 2-piperidino/2-morpholinoethyl isothiocyanate (3.05 mmol) were refluxed for 3 h. Precipitate formed was cooled, filtered and recrystallized from ethanol or isopropanol.

3.1.3.b.1. 5-{[2-(4-Chlorophenyl)-1*H*-benzimidazol-1-yl]methyl}-4-[2-(piperidin-1-yl)ethyl]-2,4-dihydro-3*H*-1,2,4-triazole-3-thione (2c)

Yield 80%, Mp: 173°C. ^{1}H NMR (400 MHz, DMSO-d_6, ppm) δ: 1.28 (brs, 6H, aliphatic H), 2.32 (brs, 4H, aliphatic H), 2.48 (t, 2H, aliphatic H), 4.09 (t, 2H, aliphatic H), 5.76 (s, 2H, CH_2), 7.28-7.30 (m, 2H, Ar-H), 7.50-7.53 (m, 1H, Ar-H), 7.64 (d, 2H, Jo= 8.4 Hz, Ar-H), 7.74 (d, 3H, Jo= 8.8 Hz, Ar-H), 13.64 (s, 1H, N-H). ^{13}C NMR (100 MHz, DMSO-d_6, ppm) δ: 23.67, 25.28, 40.22, 41.43, 54.38, 56.57, 110.94, 119.37, 122.55, 122.93, 128.50, 129.04, 130.69, 135.06, 135.78, 142.46, 148.75, 152.28, 167.36. MS (ESI+) *m/z*: 453.7(M+H), 455.5 (M+2+H). Anal. for $C_{23}H_{25}ClN_6S$-0.1H_2O (%) Calcd/Found: C 60.73/60.39; H 5.58/5.77; N 18.47/18.08; S 7.05/7.05.

3.1.3.b.2. 5-{[2-(4-Chlorophenyl)-1*H*-benzimidazol-1-yl]methyl}-4-[2-(morpholin-4-yl)ethyl]-2,4-dihydro-3*H*-1,2,4-triazole-3-thione (3c)

Yield 57%, Mp: 270-272°C. ^{1}H NMR (400 MHz, DMSO-d_6, ppm) δ: 2.37 (brs, 4H, aliphatic H), 3.30 (brs, 6H, aliphatic H), 4.09 (s, 2H, aliphatic H), 5.76 (s, 2H, CH2), 7.26-7.29 (m, 2H, Ar-H), 7.51-7.52 (m, 1H, Ar-H), 7.62-7.65 (m, 2H, Ar-H), 7.72-7.74 (m, 3H, Ar-H), 13.64 (s, 1H, N-H). ^{13}C NMR (100 MHz, DMSO-d6, ppm) δ: 40.25, 40.91, 53.40, 56.26, 65.89, 110.86, 119.31, 122.48, 122.91, 128.47, 128.96, 130.63, 134.97, 135.81, 142.42, 148.54, 152.15, 167.47. MS (ESI+) *m/z*: 455.5(M+H), 457.9(M+2+H). Anal. for $C_{22}H_{23}ClN_6OS$ (%) Calcd/Found: C 58.08/58.08; H 5.10/5.32; N 18.47/18.08; S 7.08/6.93.

3.1.3.b.3. 5-{[2-(4-Methoxyphenyl)-1*H*-benzimidazol-1-yl]methyl}-4-[2-(piperidin-1-yl)ethyl]-2,4-dihydro-3*H*-1,2,4-triazole-3-thione (6c)

Yield 75%, Mp: 158-159°C. ^{1}H NMR (400 MHz, DMSO-d_6, ppm) δ: 1.27 (brs, 6H, aliphatic H), 2.31 (brs, 4H, aliphatic H), 2.46 (t, 2H, aliphatic H), 3.81 (s, 3H, OCH_3), 4.09 (t, 2H, aliphatic H), 5.75 (s, 2H, CH_2), 7.12 (d, 2H, Jo=9.2 Hz, Ar-H), 7.21-7.27 (m, 2H, Ar-H), 7.46-7.48 (m, 1H, Ar-H), 7.63-7.70 (m, 3H, Ar-H), 13.66 (s, 1H, N-H). ^{13}C NMR (100 MHz, DMSO-d_6, ppm) δ: δ 24.16, 25.74, 40.69, 41.84, 54.84, 55.78, 57.02, 111.20, 114.81, 119.50, 122.28, 122.74, 122.87, 130.82, 136.22, 143.01, 149.38, 153.84, 161.06, 167.74. MS (ESI+) *m/z*: 449.5 (M+H). Anal. for $C_{24}H_{28}N_6OS$-0,95H_2O (%) Calcd/Found: C 61.89/61.57; H 6.47/6.23; N 18.04/17.82; S 6.88/6.81.

3.1.3.b.4. 5-{[2-(4-Methoxyphenyl)-1*H*-benzimidazol-1-yl]methyl}-4-[2-(morpholin-4-yl)ethyl]-2,4-dihydro-3*H*-1,2,4-triazole-3-thione (7c)

Yield 49%, Mp: 220°C. ^{1}H NMR (400 MHz, DMSO-d_6, ppm) δ: 2.38 (brs, 4H, aliphatic H), 3.32 (brs, 6H, aliphatic H), 3.82 (s, 3H, OCH_3), 4.11 (brs, 2H, aliphatic H), 5.76 (s, 2H, CH_2), 7.12 (d, 2H, Jo= 8.8 Hz, Ar-H), 7.24-7.26 (m, 2H, Ar-H), 7.49-7.51 (m, 1H, Ar-H), 7.66 (d, 2H, Jo= 8.8 Hz, Ar-H), 7.68-7.71 (m, 1H, Ar-H), 13.69 (s, 1H, N-H). MS (ESI+) *m/z*: 451.7 (M+H). Anal. for $C_{23}H_{26}N_6O_2S$-1,7H_2O (%) Calcd/Found: C 57.40/57.59; H 6.15/5.98; N 17.46/16.77; S 6.66/6.28.

3.1.3.b.5. 5-[(2-Phenyl-1*H*-benzimidazol-1-yl)methyl]-4-[2-(piperidin-1-yl)ethyl]-2,4-dihydro-3*H*-1,2,4-triazole-3-thione (10c)

Yield 72%, Mp: 252-254°C. ^{1}H NMR (400 MHz, DMSO-d_6, ppm) δ: 1.27 (brs, 6H, aliphatic H), 2.31 (brs, 4H, aliphatic H), 2.46 (t, 2H, aliphatic H), 4.09 (t, 2H, aliphatic H), 5.79 (s, 2H, CH2), 7.26-7.30 (m, 2H, Ar-H), 7.49-7.57 (m, 4H, Ar-H), 7.72-7.74 (m, 3H, Ar-H), 13.66 (s, 1H, N-H). ^{13}C NMR (100 MHz, DMSO-d_6, ppm) δ: 23.67, 25.29, 40.21, 41.38, 54.37, 56.51, 109.53, 110.89, 119.28, 122.41, 122.71, 128.88, 129.66, 130.01, 135.74, 142.52, 148.83, 153.35, 167.26. MS (ESI+) *m/z*: 419.3 (M+H). Anal. for $C_{23}H_{26}N_6S$ (%) Calcd/Found: C 64.88/64.73; H 6.34/6.44; N 19.73/19.49; S 7.53/7.49.

3.1.3.b.6. 5-[(2-Phenyl-1*H*-benzimidazol-1-yl)methyl]-4-[2-(morpholin-4-yl)ethyl]-2,4-dihydro-3*H*-1,2,4-triazole-3-thione (11c)

Yield 49%, Mp: 135-137.5°C. ^{1}H NMR (400 MHz, DMSO-d_6, ppm) δ: 2.36 (brs, 4H, aliphatic H), 3.33 (brs, 6H, aliphatic H), 4.10 (t, 2H, aliphatic H), 5.77 (s, 2H, CH_2), 7.26-7.29 (m, 2H, Ar-H), 7.51-7.58 (m, 4H, Ar-H), 7.72-7.74 (m, 3H, Ar-H), 13.68 (s, 1H, N-H). ^{13}C NMR (100 MHz, DMSO-d_6, ppm) δ: 40.79, 41.41, 53.94, 56.83, 66.42, 110.00, 111.38, 119.75, 122.87, 123.22, 129.36, 130.14, 130.51, 136.27, 142.98, 149.24, 153.76, 167.85. MS (ESI+) *m/z*: 421.4 (M+H). Anal. for $C_{22}H_{24}N_6OS$-1.7H_2O (%) Calcd/Found: C 58.56/58.21; H 6.12/6.23; N 18.62/18.34; S 7.10/7.02.

3.1.3.b.7. 5-{[2-(3,4-Dibenzyloxyphenyl)-1*H*-benzimidazol-1-yl]methyl}-4-[2-(piperidin-1-yl)ethyl]-2,4-dihydro-3*H*-1,2,4-triazole-3-thione (14c)

Yield 63%, Mp: 127°C. ^{1}H NMR (400 MHz, DMSO-d_6, ppm) δ: 1.23 (brs, 6H, aliphatic H), 2.26 (brs, 4H, aliphatic H), 2.45 (t, 2H, aliphatic H), 4.06 (t, 2H, aliphatic H), 5.04 (s, 2H, O$\underline{CH_2}$Ph), 5.21 (s, 2H, O$\underline{CH_2}$Ph), 5.71 (s, 2H, CH_2), 7.24-7.25 (m, 4H, Ar-H), 7.31-7.49 (m, 12H, Ar-H), 7.69 (s, 1H, Ar-H). MS (ESI+) *m/z*: 631.6 (M+H). Anal. for $C_{37}H_{38}N_6O_2S$-0,1H_2O (%) Calcd/Found: C 70.24/69.84; H 6.08/6.42; N 13.28/13.06; S 5.06/5.38.

3.1.3.b.8. 5-{[2-(3,4-Dibenzyloxyphenyl)-1*H*-benzimidazol-1-yl]methyl}-4-[2-(morpholin-4-yl)ethyl]-2,4-dihydro-3*H*-1,2,4-triazole-3-thione (15c)

Yield 38%, Mp: 187°C. ^{1}H NMR (400 MHz, DMSO-d_6, ppm) δ: 3.23 (brs, 6H, aliphatic H), 3.59 (brs, 4H, aliphatic H), 4.59 (t, 2H, aliphatic H), 5.21 (s, 2H, OCH_2Ph), 5.27 (s, 2H, OCH_2Ph), 6.18 (s, 2H, CH_2), 7.29-7.49 (m, 12H, Ar-H), 7.52-7.56 (m, 2H, Ar-H), 7.62 (s, 1H, Ar-H), 7.86 (d, 1H, Jo= 6.8 Hz, Ar-H), 8.03 (d, 1H, Jo= 7.6 Hz, Ar-H), 13.99 (s, 1H, N-H). MS (ESI+) *m/z*: 633.8 (M+H). Anal. for $C_{36}H_{36}N_6O_3S$-0.3 H_2O (%) Calcd/Found: C 67.75/67.85; H 5.78/6.15; N 13.16/12.52; S 5.02/4.76.

3.2. Pharmacology

3.2.1. EGFR Kinase Assays

ADP-Glo™ assay kit [22] evaluates kinase activity by quantifying the amount of ADP produced during a kinase reaction. The assays contained several consecutive steps. Preliminary assays were performed to determine the amount of kinase and ATP (not shown). Next a kinase reaction was performed with 5 ng EGFR kinase and 50 µM ATP. As recommended by the manufacturer, kinase reaction was the total volume of the kinase reaction was 25 µLand the amount of EGFR substrate, PolyE_4Y_1, was 1 µg based on the previously published manuscripts in the field. To terminate the kinase reaction, 25 µL ADP-Glo™ reagent was added to terminate the reaction and deplete the unused ATP. Finally, a kinase detection reagent was added to convert the ADP produced during the kinase reaction to ATP. The amount of newly synthesized ATP was determined by a luciferase/luciferin reaction.

Maximum kinase activity (100% kinase) was determined as the luminescence obtained in the kinase reaction where EGFR kinase, PolyE_4Y_1, ATP and diluting agent, 5% DMSO were present in the reaction medium. Inhibitory efficiency of each compound (with expected inhibitory activity) was determined by comparing the

enzyme activities in the presence of the inhibitors with the maximum enzyme activity. Percent inhibition was calculated based on the luminescence of the maximum activity.

3.2.2. Screening of Inhibitor Activity

Kinase reactions were performed in 25 µl reaction medium where 50 µM ATP, 5 ng EGFR kinase ± 1 µM inhibitor were present in each reaction. To confirm dose-dependency of its inhibitory activity, erlotinib was tested in two different concentrations: 100nM and 1µM to confirm of the inhibitory activity. DMSO (solvent, is used as a control in all experiments. These reactions constitute the maximum kinase activity (100% activity).

3.2.3. Cell Culture Studies

The cells were kept in high glucose (4.5 mM) DMEM that was supplemented with 10% fetal bovine serum (FBS), 2 mM L-glutamine, and 1% penicillin–streptomycin (10.000 U/mL penicillin–10.000 µg/mL streptomycin). Cells were seeded onto the 24-well tissue culture plates and kept in a 37°C incubator. MTT (3-(4,5-Dimethylthiazol-2-yl)-2,5-diphenyltetrazolium bromide) assays were employed to assess the effects of compounds 12b, 12c, 13c, 14c, 15c, 16 and 16c and erlotinib on cell viability. When the cells reached 80% confluency, the inhibitors (10µM) and erlotinib (1µM) were dissolved in DMSO and added to cells. To test for possible effects of DMSO on viability, 1 µl of DMSO was added to control cells. In addition, some wells were left untreated and incubated with regular cell culture media. MTT in phosphate buffer saline (PBS) solution was added to all cells. After incubation at 37°C for 2 h, the media was carefully removed, purple formazan crystals were dissolved in DMSO and the absorbance of the solution was determined at 550 nm. The viability of the control cells was defined as 100% and the relative cell viability (%) was calculated based on the absorbance.

3.3. *Molecular Docking*

AutoDock vina v.1.1.2 [28] was used to dock the ligands into receptor binding site. The X-ray structure of EGFR tyrosine kinase [29] in complex with erlotinib, PDB ID: 1M17, was downloaded from protein data bank (http://www.rcsb.org/pdb/home/home.do). The ligand erlotinib and other non-protein molecules were initially removed from the binding pocket. MGL Tools v.1.5.6. [30] was used to arrange the receptor and the ligands that were saved in .pdbqt format for docking. Docking of the compounds **16** and **16c** were carried out in a grid box determined by MGL Tools v.1.5.6 [30]. The most suitable poses of the docked ligands were selected based on the benzimidazole pharmacophore. Docked ligands were analyzed with UCSF Chimera-1.7 package [31].

3.4. *X-Ray Diffraction*

We determined the crystal structure of compound **5c** by X-ray diffraction. We collected the intensities of Bragg reflections which are used in determining the structure on Bruker APEX2 [32]. We used WinGX [33] program for the structural solution (SHELXS-97 [34]) and the full-matrix least squares refinement (SHELXL-97 [35]). We did the refinement of all atoms anisotropically, except for hydrogens. We found the position of the hydrogen atom of N5 in triazole ring using a difference map and refined it isotropically, on the other hand, we used riding model to calculate other hydrogen atoms idealized positions.

Crystallographic structural data of **5c** molecule have been deposited at the Cambridge Crystallographic Data Centre (CCDC) with CCDC 1854601 deposition number.

Acknowledgement: This study is partially funded by Ankara University-BAP 17H0237002 and TUBITAK 214S574. The authors acknowledge Hitit University-Scientific Research Unit (BAP) with project number FEF19004.17.001 and the Aksaray University Science and Technology Application and Research Center, Aksaray, Turkey, for the use of the Bruker SMART BREEZE CCD diffractometer (purchased under grant No. 2010K120480 of the State of Planning Organization).

References

[1] Normanno, N., De Luca, A., Bianco, C., Strizzi, L., Mancino, M., Maiello, M.R., Carotenuto, A., De Feo, G., Caponigro, F., Salomon, D.S., 2006. Epidermal growth factor receptor (EGFR) signaling in cancer. Gene 366, 2–16. https://doi.org/10.1016/j.gene.2005.10.018

[2] Bianco, R., Gelardi, T., Damiano, V., Ciardiello, F., Tortora, G., 2007. Rational bases for the development of EGFR inhibitors for cancer treatment. The International Journal of Biochemistry & Cell Biology 39, 1416–1431. https://doi.org/10.1016/j.biocel.2007.05.008

[3] Liao, B.-C., Lin, C.-C., Yang, J.C.-H., 2015. Second and third-generation epidermal growth factor receptor tyrosine kinase inhibitors in advanced nonsmall cell lung cancer: Current Opinion in Oncology 27, 94–101. https://doi.org/10.1097/CCO.0000000000000164

[4] Cheng, H., Nair, S.K., Murray, B.W., 2016. Recent progress on third generation covalent EGFR inhibitors. Bioorganic & Medicinal Chemistry Letters 26, 1861–1868. https://doi.org/10.1016/j.bmcl.2016.02.067

[5] Cheng, W., Zhou, J., Tian, X., Zhang, X., 2016. Development of the Third Generation EGFR Tyrosine Kinase Inhibitors for Anticancer Therapy. Current Medicinal Chemistry 23, 3343–3359. https://doi.org/10.2174/0929867323666160510123604

[6] Patel, H., Pawara, R., Ansari, A., Surana, S., 2017. Recent updates on third generation EGFR inhibitors and emergence of fourth generation EGFR inhibitors to combat C797S resistance. European Journal of Medicinal Chemistry 142, 32–47. https://doi.org/10.1016/j.ejmech.2017.05.027

[7] Wang, S., Song, Y., Liu, D., 2017. EAI045: The fourth-generation EGFR inhibitor overcoming T790M and C797S resistance. Cancer Letters 385, 51–54. https://doi.org/10.1016/j.canlet.2016.11.008

[8] Jia, Y., Juarez, J., Li, J., Manuia, M., Niederst, M.J., Tompkins, C., Timple, N., Vaillancourt, M.-T., Pferdekamper, A.C., Lockerman, E.L., Li, C., Anderson, J., Costa, C., Liao, D., Murphy, E., DiDonato, M., Bursulaya, B., Lelais, G., Barretina, J., McNeill, M., Epple, R., Marsilje, T.H., Pathan, N., Engelman, J.A., Michellys, P.-Y., McNamara, P., Harris, J., Bender, S., Kasibhatla, S., 2016b. EGF816 Exerts Anticancer Effects in Non–Small Cell Lung Cancer by Irreversibly and Selectively Targeting Primary and Acquired Activating Mutations in the EGF Receptor. Cancer Res 76, 1591. https://doi.org/10.1158/0008-5472.CAN-15-2581

[9] Liu, H.-B., Gao, W.-W., Tangadanchu, V.K.R., Zhou, C.-H., Geng, R.-X., 2018. Novel aminopyrimidinyl benzimidazoles as potentially antimicrobial agents: Design, synthesis and biological evaluation. European Journal of Medicinal Chemistry 143, 66–84. https://doi.org/10.1016/j.ejmech.2017.11.027

[10] Alp, M., Göker, H., Brun, R., Yıldız, S., 2009. Synthesis and antiparasitic and antifungal evaluation of 2′-arylsubstituted-1H,1′H-[2,5′]bisbenzimidazolyl-5-carboxamidines. European Journal of Medicinal Chemistry 44, 2002–2008. https://doi.org/10.1016/j.ejmech.2008.10.003

[11] Göker, H., Ayhan-Kilcigil, G., Tunçbilek, M., Kus, C., Ertan, R., Kendi, E., Özbey, S., Fort, M., Garcia, C., J. Farré, A., 1999. Synthesis and Antihistaminic H1 Activity of 1,2,5(6)-Trisubstituted Benzimidazoles. Heterocycles 51, 2561. https://doi.org/10.3987/COM-99-8585

[12] Nakano, H., Inoue, T., Kawasaki, N., Miyataka, H., Matsumoto, H., Taguchi, T., Inagaki, N., Nagai, H., Satoh, T., 2000. Synthesis and biological activities of novel antiallergic agents with 5-lipoxygenase inhibiting action. Bioorganic & Medicinal Chemistry 8, 373–380. https://doi.org/10.1016/S0968-0896(99)00291-6

[13] Hu, Z., Ou, L., Li, S., Yang, L., 2014. Synthesis and biological evaluation of 1-cyano-2-amino-benzimidazole derivatives as a novel class of antitumor agents. Medicinal Chemistry Research 23, 3029–3038. https://doi.org/10.1007/s00044-013-0888-6

[14] Akhtar, M.J., Siddiqui, A.A., Khan, A.A., Ali, Z., Dewangan, R.P., Pasha, S., Yar, M.S., 2017. Design, synthesis, docking and QSAR study of substituted benzimidazole linked oxadiazole as cytotoxic agents, EGFR and erbB2 receptor inhibitors. European Journal of Medicinal Chemistry 126, 853–869. https://doi.org/10.1016/j.ejmech.2016.12.014

[15] Demirel, S., Ayhan Kilcigil, G., Kara, Z., Güven, B., Onay Beşikci, A., 2017. Synthesis and Pharmacologic Evaluation of Some Benzimidazole Acetohydrazide Derivatives as EGFR Inhibitors. The Turkish Journal of Pharmaceutical Sciences 285–289. https://doi.org/10.4274/tjps.24008

[16] Cheong, J.E., Zaffagni, M., Chung, I., Xu, Y., Wang, Y., Jernigan, F.E., Zetter, B.R., Sun, L., 2018. Synthesis and anticancer activity of novel water soluble benzimidazole carbamates. European Journal of Medicinal Chemistry 144, 372–385. https://doi.org/10.1016/j.ejmech.2017.11.037

[17] Kuş, C., Ayhan-Kılcıgil, G., Özbey, S., Kaynak, F.B., Kaya, M., Çoban, T., Can-Eke, B., 2008. Synthesis and antioxidant properties of novel N-methyl-1,3,4-thiadiazol-2-amine and 4-methyl-2H-1,2,4-triazole-3(4H)-thione derivatives of benzimidazole class. Bioorganic & Medicinal Chemistry 16, 4294–4303. https://doi.org/10.1016/j.bmc.2008.02.077

[18] Ayhan-Kılcıgil, G., Gürkan, S., Çoban, T., Özdamar, E.D., Can-Eke, B., 2012. Synthesis and Evaluation of Antioxidant Properties of Novel 2-[2-(4-chlorophenyl) benzimidazole-1-yl]-N-(2-arylmethylene amino) acetamides and 2-[2-(4-chlorophenyl) benzimidazole-1-yl]-N-(4-oxo-2-aryl-thiazolidine-3-yl) acetamides-I: Synthesis and Evaluation of Antioxidant Properties. Chemical Biology & Drug Design 79, 869–877. https://doi.org/10.1111/j.1747-0285.2012.01347.x

[19] Ayhan-Kilcigil, G., Kuş, C., Çoban, T., Özdamar, E.D., Can-Eke, B., 2014. Identification of a Novel Series of *N* -Phenyl-5-[(2-phenylbenzimidazol-1-yl)methyl]-1,3,4-oxadiazol-2-amines as Potent Antioxidants and Radical Scavengers: *N* -Phenyl-5-[(2-phenylbenzimidazol-1-yl)methyl]-1,3,4-oxadiazol-2-amines. Archiv der Pharmazie 347, 276–282. https://doi.org/10.1002/ardp.201300324

[20] Xu, X., 2015. Parallel phase 1 clinical trials in the US and in China: accelerating the test of avitinib in lung cancer as a novel inhibitor selectively targeting mutated EGFR and overcoming T790M-induced resistance. Chinese Journal of Cancer 34. https://doi.org/10.1186/s40880-015-0029-3

[21] Zhang, H., 2016. Osimertinib making a breakthrough in lung cancer targeted therapy. OncoTargets and Therapy Volume 9, 5489–5493. https://doi.org/10.2147/OTT.S114722

[22] ADP-Glo™ Kinase Assay. Technical Manual. Promega, https://www.promega.com/-/media/files/resources/protocols/technical-manuals/101/adp-glo-lipid-kinase-assay-protocol.pdf

[23] ATCC Product characteristics. https://www.lgcstandards-atcc.org/Products/All/HTB-22.aspx?geo_country=tr#generalinformation.

[24] Subik, K., Lee, J.-F., Baxter, L., Strzepek, T., Costello, D., Crowley, P., Xing, L., Hung, M.-C., Bonfiglio, T., Hicks, D.G., Tang, P., 2010. The Expression Patterns of ER, PR, HER2, CK5/6, EGFR, Ki-67 and AR by Immunohistochemical Analysis in Breast Cancer Cell Lines. Breast Cancer: Basic and Clinical Research 4, 117822341000400. https://doi.org/10.1177/117822341000400004

[25] Abdelgawad, M.A., Bakr, R.B., Alkhoja, O.A., Mohamed, W.R., 2016. Design, synthesis and antitumor activity of novel pyrazolo[3,4-d]pyrimidine derivatives as EGFR-TK inhibitors. Bioorganic Chemistry 66, 88–96. https://doi.org/10.1016/j.bioorg.2016.03.011

[26] Johnson, C.K., 1965. ORTEP, Report ORNL-3794, Oak Ridge National Laboratory, Tenessee, USA.
[27] Ayhan-Kılcıgil, G., Kus, C., Özdamar, E.D., Can-Eke, B., Iscan, M., 2007. Synthesis and Antioxidant Capacities of Some New Benzimidazole Derivatives. Archiv der Pharmazie 340, 607–611. https://doi.org/10.1002/ardp.200700088
[28] Trott, O., Olson, A.J., 2009. AutoDock Vina: Improving the speed and accuracy of docking with a new scoring function, efficient optimization, and multithreading. Journal of Computational Chemistry NA-NA. https://doi.org/10.1002/jcc.21334
[29] Stamos, J., Sliwkowski, M.X., Eigenbrot, C., 2002. Structure of the Epidermal Growth Factor Receptor Kinase Domain Alone and in Complex with a 4-Anilinoquinazoline Inhibitor. Journal of Biological Chemistry 277, 46265–46272. https://doi.org/10.1074/jbc.M207135200
[30] Sanner,M.F., 1999, Python: A Programming language for software integration and development. J. Mol. Graphics Mod. 1-7. https://www.scripps.edu/sanner/html/papers/NewsAndViewsSept99.pdf
[31] Pettersen, E.F., Goddard, T.D., Huang, C.C., Couch, G.S., Greenblatt, D.M., Meng, E.C., Ferrin, T.E., 2004. UCSF Chimera?A visualization system for exploratory research and analysis. Journal of Computational Chemistry 25, 1605–1612. https://doi.org/10.1002/jcc.20084
[32] Bruker (2012), APEX2, SAINT and SADABS, Bruker AXS Inc, Madison, Wisconsin, USA.
[33] Farrugia, L.J., 1999. *WinGX* suite for small-molecule single-crystal crystallography. Journal of Applied Crystallography 32, 837–838. https://doi.org/10.1107/S0021889899006020
[34] Sheldrick, G. M., 1997. SHELXS97, Univ. of Göttingen, Germany.
[35] Sheldrick, G. M., 1997. SHELXL97, Univ. of Göttingen, Germany.

30 New compounds with benzimidazole scaffolds were designed and synthesized.

Crystal and molecular structure of the compound **5c** has been characterized by single crystal X-ray crystallographic analysis.

EGFR kinase inhibitory potencies of synthesized compounds were compared with erlotinib *in vitro.*

Docking was carried for three compounds by using the X-ray structure of EGFR tyrosine kinase.